Delicate and robust dynamical recurrences of matter waves in driven optical crystals

Muhammad Ayub*[1,2] and Farhan Saif†[1,3]

[1]*Department of Electronics, Quaid-i-Azam University, 45320, Islamabad, Pakistan.*
[2]*Theoretical Plasma Physics Division, PINSTECH, Nilore, 45650, Islamabad, Pakistan.*
[3]*Center for Applied Physics and Mathematics, National University of Science and Technology, Islamabad, Pakistan.*

We study dynamical recurrences of a Bose-Einstein condensate in an optical crystal subject to a periodic external driving force. The recurrence behavior of the condensate is analyzed as a function of time close to nonlinear resonances occurring in the classical counterpart. Our mathematical formalism for the recurrence time scales is presented as *delicate recurrences,* which take place, for instance when the lattice is perturbed weakly and *robust recurrences,* which may manifest themselves for a sufficiently strong external driving force. The analysis not only is valid for a dilute condensate, but also is applicable for strongly interacting homogeneous condensate provided; the external modulation causes no significant change in density profile of the condensate. We explain parametric dependence of the dynamical recurrence times which can easily be realized in laboratory experiments. In addition, we find a good agreement between the obtained analytical results and numerical calculations.

PACS numbers: 67.85.Hj, 42.65.Sf, 03.75.-b

I. INTRODUCTION

Coherent control of matter waves is at the heart of many theoretical and experimental interests. Coherence of matter waves in optical crystals has evolved as an active research area over last two decades and led to analyze fundamental characteristics of quantum mechanics [1], quantum tunneling [2], Bloch oscillations [3], quantum information [4] and quantum chaos[5, 6]. The fascinating developments in this subject have wide applications from quantum metrology [7] to quantum corrals [8]. Time periodic modulations in matter wave optics have given birth both to hybrid nano-opto-mechanical systems [9] and driven billiards [10]. Hence, the theoretical and experimental advancements have led to explore coherent transport [11, 12], controlling ratchet effects [13], dynamical localization [14, 15], coherent destruction of tunneling [16], photon assisted tunneling [17], entanglement [18], precision measurement of gravitational acceleration [19] and extracting nearest-neighbor spin correlations in a fermionic Mott insulator [20] in driven optical crystals. Furthermore, realization of strongly correlated phases [21], coherent acceleration of matter wave [22] in driven optical crystals [23] have been studied in great details.

A quantum particle in its early evolution in a bounded system follows classical mechanics and reappears after a classical period following classical trajectory. Later, following wave mechanics, it spreads and collapses as a consequence of non-linearity of the energy spectrum. However, the discreteness of the quantum mechanics leads to its reconstruction at various longer time scales, which define quantum recurrence times, such as, quantum revival time and supper revival time. We explain these recurrences of a quantum particle in a quantum chaotic system, which manifests complex dynamics in its classical counterpart. Due to their dependence on modulation effects, these dynamical recurrences are different from those taking place in an undriven system, and may be considered as a probe to study quantum chaos [24]. Dynamical recurrences, in a bounded driven system, originate from the simultaneous excitation of discrete quasi-energy states [25, 26]. In the present paper we explain matter waves dynamics in a phase modulated optical crystal and provide analytical relations for classical period, quantum revival and super-revival time scales. In addition, we explain the existence of delicate dynamical recurrences, for weak effective modulation, and robust dynamical recurrences for strong effective modulation of the periodically driven optical crystal. The classical counterpart of the dynamical system displays dominant regular dynamics and dominant stochastic dynamics, one after the other, as a function of increasing modulation amplitude [6]. Our analysis is valid for weakly interacting BECs, a situation that can be realized experimentally with Feshbach scattering resonances [27]. In addition, we suggest that the analysis is valid for strongly interacting homogeneous condensates as well, where, nonlinear term can be replaced by an effective potential provided the external modulation causes slight changes in density profile of the condensate as discussed in Ref. [28]. Hence, due to spatial and temporal periodicity in the driven optical crystal, the quantum dynamics of the condensate inside a nonlinear resonance is effectively mapped on the Mathieu equation. Our analytical findings are confirmed by numerical results.

The paper is organized as follows: In Sec. II, we model the effective Hamiltonian governing the time evolution. Later, the quasi-energy spectrum for nonlinear

*ayubok@gmail.com
†farhan@qau.edu.pk

resonances in periodically driven optical crystal is explained. We obtain mathematical relations for recurrence time scales for the two cases; delicate dynamical recurrences and robust dynamical recurrences for matter waves in driven optical crystal in Sec. III. The analytical and numerical results are summarized in Sec. IV.

II. THE MODEL

We consider a condensate which is loaded in the lower edge of the band corresponding to optical crystal to avoid dynamical and Landau instabilities [29]. The dynamics of the matter wave in driven one dimensional optical crystal, strongly confined by radial trap is governed by the Hamiltonian [15, 30],

$$H = \frac{p^2}{2M} + \frac{\tilde{V}_o}{2}\cos[2k_L\{x - \Delta L\sin(\omega_m t)\}] + g_{1D}|\tilde{\psi}|^2,$$

where, k_L is wave number, $\tilde{V}_o$ defines the potential depth of the lattice. Moreover, ΔL and ω_m are respectively, amplitude and frequency of external drive, whereas, M is the mass of an atom. Furthermore, $g_{1D} = \hbar k_L \omega_\perp a_s$ defines the effective two body interaction coefficient, $\omega_\perp$ is radial trap frequency and a_s is inter-atomic s-wave scattering length.

The unitary transformation[1] $\tilde{\psi} = \psi(x,t)\exp[\frac{i}{\hbar}\{\omega_m M\Delta L\cos(\omega_m t)x + \beta(t)\}]$, (where, $\beta(t) = \frac{\omega_m^2\Delta L^2 M}{4}[\frac{\sin(2\omega_m t)}{2\omega_m} + t]$), for a frame co-moving with the lattice, modifies the Hamiltonian as

$$H = \frac{p^2}{2M} + \frac{\tilde{V}_o}{2}\cos 2k_L x - Fx\sin\omega_m t + g_{1D}|\psi|^2. \quad (1)$$

Here, $F = M\Delta L\omega_m^2$ is amplitude of inertial force emerging in the oscillating frame. To examine the dynamics of cold atoms in driven optical crystals numerically, Hamiltonian (1) is expressed in dimensionless quantities. We scale the quantities so that $z = k_L x$, $\tau = \omega_m t$, $\psi = \frac{\psi}{\sqrt{n_0}}$, where, $\sqrt{n_0}$ is average density of a condensate. Multiplying the Schrödinger wave equation by $\frac{2\omega_r}{\hbar\omega_m^2}$, where, $\omega_r = \frac{\hbar k_L^2}{2M}$ is single photon recoil frequency, we get dimensionless Hamiltonian, viz

$$\tilde{H} = -\frac{\bar{k}^2}{2}\frac{\partial^2}{\partial z^2} + \frac{V_o}{2}\cos 2z + \lambda z\sin\tau + G|\psi|^2. \quad (2)$$

Here, $G = \frac{g_{1D}n_0\bar{k}}{\hbar\omega_m}$, and $\lambda = \frac{F\ d_L\ \bar{k}}{\hbar\omega_m} = k_L\Delta L$ is scaled modulation amplitude. Also $V_o = \frac{\tilde{V}_o\bar{k}}{2\hbar\omega_m}$, τ is scaled time in the units of modulation frequency, ω_m, and d_L defines the periodicity of optical crystal. In this case, the rescaled Planck's constant is $\bar{k} = \frac{2\omega_r}{\omega_m}$.

[1] The unitary transformation is time periodic and preserves the quasi-energy spectrum.

For the dynamics of weakly interacting BECs in optical crystal the interaction term can safely be neglected [14], which is a situation achievable in the present day experiments with the advent of Feshbach scattering resonances. In addition, the effective potential $\frac{V_o}{2}\cos 2z + G|\psi|^2$ seen by each atom may as well be written [28] as,

$$V_{eff} = \frac{\acute{V}}{2}\cos(2z) + const,$$

where, $\acute{V} = \frac{V_o}{1+4G}$.

The analytical result, calculated using perturbation theory [28], is valid as long as the condensate density is nearly uniform, i.e. , $\acute{V} << 1$ which describes either a weak external potential V_o or a strong atomic interaction G. The condition is experimentally confirmed for one dimensional potential [31]. The effective dynamics of matter wave in this regime is governed by the Hamiltonian

$$\tilde{H} = -\frac{\bar{k}^2}{2}\frac{\partial^2}{\partial z^2} + \frac{\acute{V}}{2}\cos 2z + \lambda z\sin\tau. \quad (3)$$

Here and onward $\acute{V}$ is expressed in the units of recoil energy $E_r = \hbar\omega_r$.

In order to understand the classical dynamics of the system, we plot the Poincaré surface of section for shallow optical crystal ($\acute{V} = 2$) with modulation strengths $\lambda = 0,\ 0.5,\ 1$ and for deep lattice ($\acute{V} = 16$) with modulation strengths $\lambda = 0,\ 0.5,\ 1.5$ as shown in Fig. 1. From phase space plot, we see the appearance of 1:1 resonance for $\lambda > 0$. This resonance emerges when the time period of external force matches with period of unperturbed system. One effect of an external modulation is the development of stochastic region near the separatrix. As modulation is increased, while the frequency is fixed, the size of stochastic region increases at the cost of regular region.

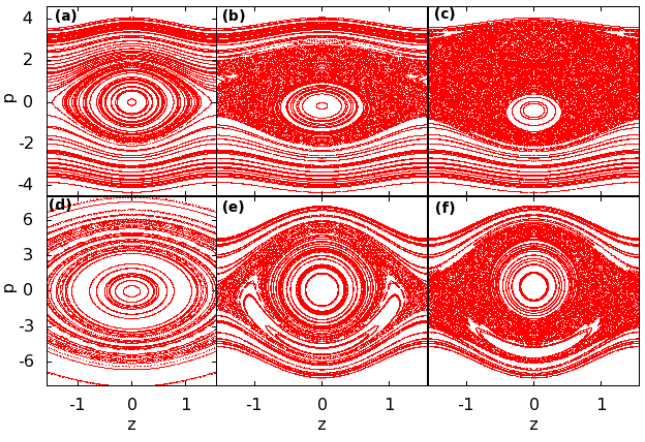

FIG. 1: Poincare phase space for different modulation strengths and lattice potentials. Upper row: $\lambda = 0$, (a) ,0.5, (b) 1.5, (c) and $\acute{V} = 2$; Lower row: $\lambda = 0$, (d) 0.5, (e) 1.5, (f) and $\acute{V} = 16$.

In order to solve the time dependent Schrödinger equation near the nonlinear resonances of the driven quantum system corresponding to the Hamiltonian (2), we [32–34], provide an ansatz as

$$|\psi(t)\rangle = \sum_n C_n(t)|n\rangle \exp[-i\{E_{\bar{n}} + (n-\bar{n})\frac{\hbar}{N}\}\frac{t}{\hbar}], \quad (4)$$

where, $E_{\bar{n}}$ is the mean energy, $C_n(t)$ is time dependent probability amplitude, $\bar{n}$ is mean quantum number, $|n\rangle$ are eigen states of undriven system and N is resonance number.

The Floquet energy spectrum for nonlinear resonances is given as [35, 36],

$$\mathcal{E}_{\mu,\nu} = \left[\frac{N^2\hbar^2\zeta}{8}a_\nu(\mu(j),q) + \hbar\tilde{\alpha}j\right] \mod \hbar\omega_m, \quad (5)$$

where, $a_\nu(\mu(j),q)$ is Mathieu characteristics parameter and $q = \frac{\lambda}{\beta_0}$ is the effective modulation. Here, $\beta_0 = \frac{N^2\hbar^2\zeta}{4V}$, and $V =< n|z|n \pm 1 >$ are matrix elements and are considered constant at potential minima. The solutions are defined by π-periodic Floquet states, *i. e.* $P_\mu(\theta) = P_\mu(\theta+\pi)$, and μ is the characteristic exponent. In order to have π-periodic solutions, we require μ to be defined as $\mu = \mu(j) = 2j/N$, where, $j = 0, 1, 2, ..., N-1$.

The allowed values of $\mu(j)$ can exist as a characteristic exponent of solution to the Mathieu equation for discrete ν (which takes integer values) only for certain value $a_\nu(\mu(j),q)$, when q is fixed. The index ν takes the definition $\nu = \frac{2(n-\bar{n})}{N}$. Moreover, $\tilde{\alpha}$ defines the winding number. For driven optical potential, keeping the periodicity of Floquet solutions [34], we take only even values of the index [37]. Hence, the re-scaled Mathieu characteristic exponent becomes

$$\nu = 2(l+\beta), \text{ where, } \beta = \frac{N\omega - 1}{N^2\zeta\hbar}. \quad (6)$$

Comparing the coefficients of eigen energy of the undriven system and equation of motion of probability amplitude in the absence of modulation, we get $l = \frac{n-\bar{n}}{N}$, which is new band index for nonlinear resonance and at the center of resonance $l = 0$. Analytical expressions of $a_\nu(\mu(j),q)$ for two asymptotic cases i.e. for $q \lesssim 1$ and $q \gg 1$ are different [37]. We discuss these two cases in Sec-III separately.

III. RECURRENCE TIMES IN A DRIVEN OPTICAL LATTICE

As recurrence time scales of driven optical crystal are expressed in terms of undriven system, we present classical period, quantum revival time and super revival time scales of matter wave in undriven optical crystal [38, 39].

In the absence of external forcing, the crystal potential replaced with effective potential in equation (1) is governed by the Hamiltonian

$$\tilde{H} = \frac{p^2}{2} + \frac{\acute{V}}{2}\cos 2z. \quad (7)$$

The corresponding time independent Schrödinger equation is eventually a Mathieu equation, where, $q_0 = \frac{\acute{V}}{4}$, is effective crystal potential scaled by recoil energy. In shallow lattice potential limit, i.e. $q_o \lesssim 1$, the classical frequency, $\omega = 2\bar{n}\{1 - \frac{q_o^2}{2(\bar{n}^2-1)^2}\}$ and non-linearity, $\zeta = 2 + \frac{q_o^2}{2}\frac{3\bar{n}^2+1}{(\bar{n}^2-1)^3}$. The classical period of the condensate is inversely proportional to the average classical frequency, ω, and calculated [38] as

$$T_0^{(cl)} = \left\{1 + \frac{q_o^2}{2(\bar{n}^2-1)^2}\right\}\frac{\pi}{\bar{n}}. \quad (8)$$

In the long time evolution the condensate spreads and observes a collapse as a result of destructive interference of constituent wavelets. At longer time the constructive interference overcomes and leads to reconstruction of the condensate at quantum revival time, that is inversely proportional to the nonlinearity of the spectrum present around the mean quantum number, $\bar{n}$, viz.

$$T_0^{(rev)} = 2\pi\left\{1 - \frac{q_o^2}{2}\frac{(3\bar{n}^2+1)}{(\bar{n}^2-1)^3}\right\}. \quad (9)$$

Whereas, the super-revival time, obtained as,

$$T_0^{(spr)} = \frac{\pi(\bar{n}^2-1)^4}{q_o^2\bar{n}(\bar{n}^2+1)}, \quad (10)$$

is inversely proportional to incremental change in nonlinearity with respect to quantum number n, at mean quantum number $\bar{n}$.

In deep optical potential limit, i.e. $q_o >> 1$, the classical frequency is $\omega = 4(\sqrt{q_o} - \frac{2\bar{n}+1}{8})$ and non-linearity is $\zeta = |-1 - \frac{3(2\bar{n}+1)}{2^4\sqrt{q_o}}|$. In this case, the classical time period, quantum revival time and super revival time are, respectively, calculated as

$$T_0^{(cl)} = \frac{\pi}{2\sqrt{q_o}}\left\{1 + \frac{s}{8\sqrt{q_o}} + \frac{3(s^2+1)}{2^8 q_o}\right\}, \quad (11)$$

$$T_0^{(rev)} = 4\pi\left(1 - \frac{3s}{16q_o}\right), \quad (12)$$

$$\text{and} \quad T_0^{(spr)} = 32\pi\sqrt{q_o}, \quad (13)$$

where, $s = 2\bar{n}+1$.

In the following we explain the quantum recurrences of condensate in optical crystal in the presence of external periodic forcing. For the sake of clarity and simplicity, we classify our later discussion as delicate dynamical recurrences for $q \lesssim 1$ and robust dynamical recurrences for $q >> 1$.

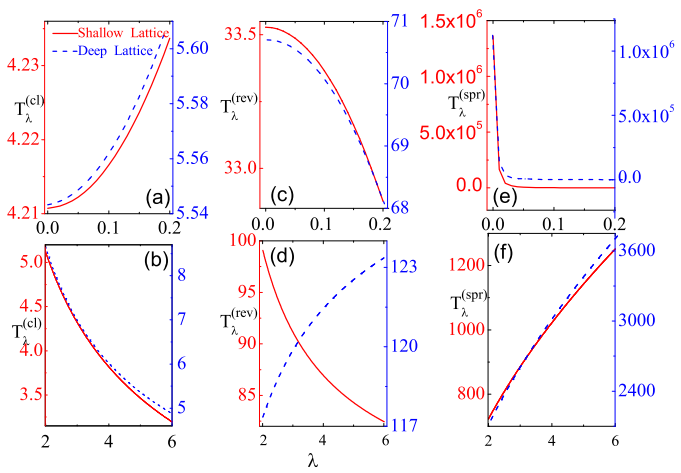

FIG. 2: Left panel: Classical time period versus $\lambda = \frac{q}{\beta_0}$ for weak external modulation (a) and for strong external modulation (b), where, $\beta_0 = \frac{\hbar^2\zeta}{4V}$ for $N = 1$. Middle panel: Quantum revival time versus λ for weak external modulation (c) and for strong external modulation (d). Right panel: Super revival time versus λ when external modulation is weak (e) and for strong external modulation (f). In this figure, for deep lattice $\acute{V} = 16$, for shallow lattice $\acute{V} = 2$ and $\hbar = 0.5$.

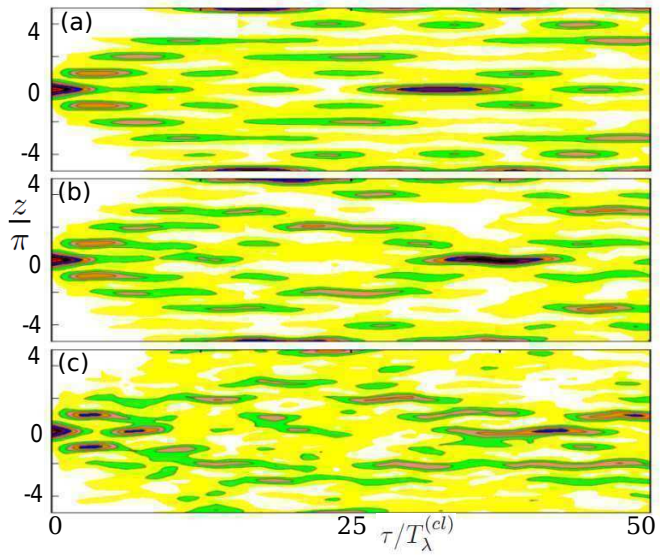

FIG. 3: Spatio-temporal behavior of atomic condensate for $q = 0(\lambda = 0)$, $\acute{V} = 2$ (a) $q = 0.2\beta_0$, $\acute{V} = 2$(b) and $q = 0.2\beta_0$, $\acute{V} = 0.3$ (c). Other parameters are $\Delta p = 0.5$, $\beta_0 = \frac{\hbar^2\zeta}{4V}$ and $\hbar = 1$.

A. Delicate dynamical recurrences

For weakly driven, shallow or deep, lattice ($q \lesssim 1$) the recurrence time scales, $T_\lambda^{(cl)}$, $T_\lambda^{(rev)}$ and $T_\lambda^{(spr)}$ for primary resonance $N = 1$ are calculated as [35]

$$T_\lambda^{(cl)} = T_0^{(cl)}\left[1 + \frac{q^2}{2}\frac{1}{\{4(l+\beta)^2 - 1\}^2}\right]\Delta, \tag{14}$$

$$T_\lambda^{(rev)} = T_0^{(rev)}\left[1 - \frac{q^2}{2}\frac{12(l+\beta)^2 + 1}{\{4(l+\beta)^2 - 1\}^3}\right], \tag{15}$$

$$\text{and} \quad T_\lambda^{(spr)} = \frac{\pi\{4(l+\beta)^2 - 1\}^4}{2\zeta\hbar q^2(l+\beta)\{4(l+\beta)^2 + 1\}}, \tag{16}$$

where, $\Delta = (1 - \frac{1}{N\omega})^{-1}$. Here, time scales for weakly driven shallow lattice and weakly driven deep lattice are similar in structure, however, they differ due to different energy spectra corresponding to undriven crystal in the two cases which leads to different undriven time scales.

In order to observe the dynamics of a condensate inside a resonance, we evolve a well localized Gaussian condensate in the driven optical crystal. Numerical results are obtained by placing a condensate in a primary resonance with $N = 1$.

The classical period time, quantum revival time and super revival time of matter waves in modulated optical crystal near nonlinear resonances versus scaled modulation $\lambda = \frac{q}{\beta_0}$ is shown in Fig. 2. In each plot of the figure, left vertical axis shows the time scale when shallow optical crystal is modulated and right axis shows the time scale when deep optical crystal is modulated. The upper row of Fig. 2 represents the time scales for small q values i.e. delicate dynamical recurrences as a function of modulation λ, whereas, lower row represents the time scales when $q \gg 1$, as a function of modulation λ, i.e. robust dynamical recurrences. Here, left column shows the results related to the classical periods. Quantum revival times are plotted in middle column, whereas, right column shows super revival times.

We note that when optical crystal is perturbed by weak periodic force, the classical period increases with modulation, as given in equation (14). Classical period for weakly driven shallow lattice potential changes slowly as compared to weakly driven deep lattice potential as shown in Fig. 2a. Quantum revival time in nonlinear resonances versus modulation is shown in middle column of Fig. 2. For delicate dynamical recurrences (Fig. 2c), the quantum revival time decreases as modulation increases. The behavior of quantum revival time is given by equation (15) for delicate dynamical recurrence. For weakly driven shallow optical crystal or weakly driven deep lattice, qualitative and quantitative behavior of revival time is almost similar. Classical period and quantum revival time for delicate dynamical recurrences show good numerical and analytical resemblance for the system with our previous work [25, 26, 40].

Fig. 3 shows spatio-temporal evolution of an initially well localized condensate in a crystal potential well. Fig. 3a is spatio-temporal dynamics in undriven crystal, while Fig. 3b & Fig. 3c present the case, for external modulation $q = 0.2\beta_0$ and different value of $\acute{V}$. Spatio-temporal

evolution of the condensate in optical crystal shows that condensate diffuses to the neighboring lattice sites by tunneling and splits into smaller wavelets. Later, these wavelets constructively interfere and condensate revival takes place. Revival time calculated numerically is the same as obtained from analytical results. Keeping modulation constant as $q = 0.2\beta_0$ but for different $\acute{V}$, which may be a consequence of varied atom-atom interaction, revival time is modified. We note that in the absence of interaction term, G, revival time changes with $\acute{V}$ and interference pattern is similar. But with the introduction of interaction term not only revival time is modified due to change in $\acute{V}$, interference pattern is also modified as seen in Fig. 3c.

B. Robust dynamical recurrences

On the other hand, for strongly driven optical crystal, the effective modulation, $q \gg 1$. Time scales for the atomic condensate for primary resonance with $N = 1$ are given as [35]

$$T_\lambda^{(cl)} = \frac{2\pi}{\hbar\zeta\left\{\sqrt{q} - \frac{4(l+\beta)+1}{8}\right\}}, \tag{17}$$

$$T_\lambda^{(rev)} = \frac{8\pi}{\hbar\zeta}\left[1 - \frac{3\{4(l+\beta)+1\}}{16\sqrt{q}}\right], \tag{18}$$

and

$$T_\lambda^{(spr)} = \frac{32\pi\sqrt{q}}{\hbar\zeta}. \tag{19}$$

In case of strongly driven crystal, when external modulation frequency is close to the harmonic frequency, matrix elements, V can be approximated by those of harmonic oscillator and effective modulation, q, can be approximated as $q \approx \frac{4\sqrt{n+1}\lambda}{q_o^{\frac{1}{4}}\hbar^2\zeta}$ [39] . Under this approximation the time scales are

$$T_\lambda^{(cl)} = \frac{16\pi q_o^{\frac{1}{8}}/\sqrt{\zeta}}{16(\bar{n}+1)^{\frac{1}{4}}\sqrt{\lambda} - \{4(l+\beta)+1\}q_o^{\frac{1}{8}}\hbar\sqrt{\zeta}}, \tag{20}$$

$$T_\lambda^{(rev)} = \frac{8\pi}{\hbar\zeta}\left[1 - \frac{3\{4(l+\beta)+1\}q_o^{\frac{1}{8}}\hbar\sqrt{\zeta}}{32(\bar{n}+1)^{\frac{1}{4}}\sqrt{\lambda}}\right],$$

and

$$T_\lambda^{(spr)} = \frac{64\pi(\bar{n}+1)^{\frac{1}{4}}\sqrt{\lambda}}{\hbar^2\zeta^{\frac{3}{2}}q_o^{\frac{1}{8}}}. \tag{21}$$

When lattice is strongly modulated by an external periodic force, the classical period decreases as modulation increases. Classical period for strongly driven optical crystal is given by equation (17). The behavior of classical period for strongly driven lattice versus modulation is qualitatively of the same order for both strongly driven shallow lattice and strongly driven deep lattice as shown in Fig. 2b. The behavior of classical period in strongly driven crystal case is understandable as strong modulation influence more energy bands of undriven crystal to follow the external frequency and near the center of nonlinear resonance the energy spectrum is almost linear [35] with assumptions $q \gg 1$ and l is small, i.e. condensate is placed near the center of resonance.

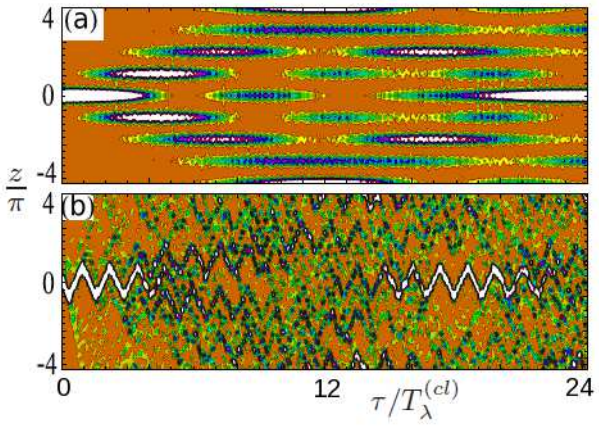

FIG. 4: Spatiotemporal behavior of atomic condensate. Wave packet dynamics in the absence of modulation (a),and in the presence of modulation when $q = 3\beta_0$ (b). Other parameters are $\acute{V} = 0.36$, $\Delta p = 0.1$ and $\hbar = 0.16$

.

Quantum revival time in nonlinear resonances versus modulation is shown in middle column of Fig. 2. For robust dynamical recurrences, the behavior of quantum revival time is given by equation (18). The qualitative behavior of revival time for strongly driven shallow lattice is different from that of strongly driven deep lattice Fig. 2d, as in the later case, change in revival time is almost one order of magnitude larger than the former case, for equal changes in modulation. Here, the difference in the revival time behavior for strongly driven shallow lattice as compared to strongly driven deep lattice is due to the difference in energy spectrum of undriven system. In deep lattice, due to small non-linearity more energy bands are influenced by the external drive and resonance spectrum is similar to that of harmonic oscillator near the center of nonlinear resonance. As modulation is increased more and more energy bands are influenced by external drive. Fig. 4 shows spatio-temporal evolution of an initially well localized wave packet in a lattice potential well inside a resonance for $\acute{V} = 16$. Fig. 4a is for the spatio-temporal dynamics of atomic condensate in the absence of periodic modulation, while Fig. 4b presents the case when external modulation, $q = 3\beta_0$. The quantum revival times in Fig. 4 seen numerically are the same as obtained analytically in equation (18).

The behavior of super revival time versus modulation is shown in right column of Fig. 2. For robust dynamical recurrences, equation (19) gives the time scale for super revivals. The super revival time for robust dynamical recurrences increases with modulation, as shown in the Fig. 2f. Here, qualitative behavior of super revival time is same for strongly driven shallow lattice and strongly driven deep lattice but quantitatively super revival time increases almost two times faster.

Square of auto-correlation function ($\mid A(t) \mid^2$) for the minimum uncertainty condensate is plotted as a function of time in Fig. 5 and Fig. 6 for $q = 0.5\beta_0$ and $q = 1.5\beta_0$ respectively. Other parameters are $\Delta p = \Delta z = 0.5$, $\hbar = 0.5$ and $\acute{V} = 16$. In these figures upper inset is an enlarged view which displays classical periods, while lower inset of the figures show quantum revivals. Lower panel shows the existence of super revivals. The classical period, quantum revival time and super revival time are indicated by arrows and showing there characteristics. Numerical results are in good agreement with analytical expressions.

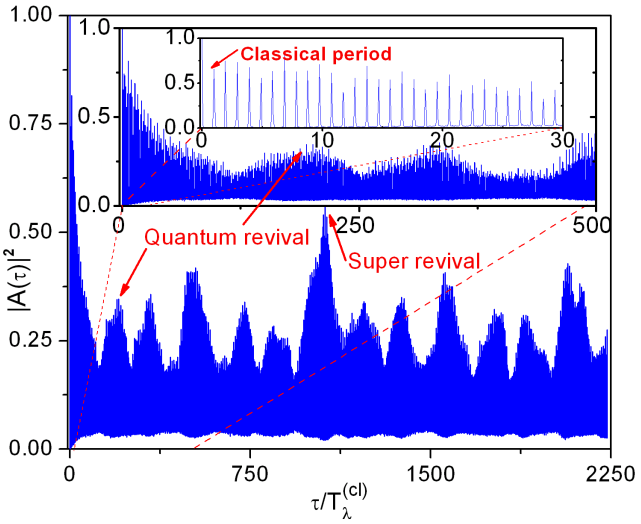

FIG. 5: Square of auto-correlation function of Gaussian condensate plotted as a function of scaled evolution time. Here, $q = 0.5\beta_0$, $\hbar = 0.5$, $\acute{V} = 16$, $\Delta z = \Delta p = 0.5$ and condensate is initially, well localized at the central lattice well around the lowest band of undriven crystal. Classical period, revival time and super revival time are indicated by arrows.

IV. DISCUSSION

We presented above a discussion on the occurrence of delicate and robust dynamical recurrences of matter wave in optical crystal in the presence of periodic modulation. The delicate dynamics condition, i. e., $q \lesssim 1$ is satisfied when shallow or deep potential is slightly perturbed by small external periodic force. Classical periods of a condensate initially localized near the center of resonance

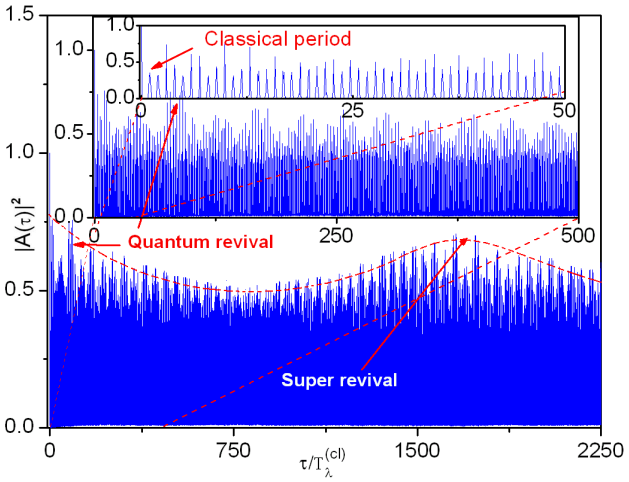

FIG. 6: Square of auto-correlation function of Gaussian condensate is plotted versus scaled time. Here, $q = 1.5\beta_0$, other parameters and conditions are same as in Fig. 5

increases with modulation for delicate dynamics. While, quantum revivals and super revivals decrease with modulation. Similarly, condition $q \gg 1$ can be satisfied for example when shallow or deep potential is strongly modulated. Classical periods in robust case decrease and super revival times increase with increasing modulation. Here, quantum revival time for the case when deep lattice is strongly modulated increases with modulation, while, it decreases when shallow is strongly modulated. The difference in the behavior is due to the contrast in energy spectrum of undriven crystals. When modulation is increased in deep lattice case more and more energy levels are influenced by external modulation (Fig. 1e, 1f), non-linearity near the center of resonance decreases and revival time increases.

Parametric dependence of analytical results are confirmed by exact numerical solutions both for delicate and robust dynamical recurrences. Both spatio-temporal (Fig. 3 and Fig. 4) and temporal (Fig. 5 and Fig. 6) dynamics show that the non-linearity of the un-driven system, and the initial conditions on the excitation contribute to the quantum revival time and super revival time.

The suggested theoretical results may be realized in experimental set up of recently performed experiments at Pisa [41], where, dynamical control of matter wave tunneling is studied in strongly shaken crystal. A BECs of about 5×10^4 ^{87}Rb atoms was evolved in a dipole trap which was realized using two intersecting Gaussian laser beams at 1030 nm wavelength and a power of around 1 W per beam focused to waists of 50 μm. After obtaining pure condensates trap beams were readjusted to obtain elongated condensates with the trap frequencies (80 Hz in radial and $\approx$ 20 Hz in the longitudinal direction). Along the axis of one of the dipole trap beams a one-dimensional optical crystal potential was introduced and the power of the lattice beams ramped up in 50 ms in order to avoid

excitations of the BEC. The optical crystals used was created using two counter-propagating Gaussian laser beams ($\lambda_L = 852\,\mathrm{nm}$) with $120\,\mu$m waist and a resulting optical crystal spacing $d_L = \lambda_L/2 = 0.426\,\mu$m. The depth V_o of the resulting periodic potential is measured in units of $E_\mathrm{r} = \hbar^2\pi^2/(2Md_L^2)$. In laboratory, accessible scaled optical lattice depth $\acute{V}$ ranges from 1 to 20.

For optical crystal with potential depth $\acute{V} = 2$, and $\acute{V} = 16$, the mean separation of the two lowest bands is $\approx 3.15kHz$ and $20.784kHz$, respectively. For the driving frequency, $\omega_m/2\pi$, ranging from $3kHz - 9kHz$, the rescaled Planck's constant $\bar{k}$ ranges from 0.668 to 2.066.

V. ACKNOWLEDGEMENT

M. A. Thanks HEC Pakistan for financial support through grant no. 17-1-1(Q.A.U)HEC/Sch/2004/5681. F. S. thanks HEC Pakistan for partial financial support under NRP-20-1374.

[1] I. Bloch, J. Dalibard, and W. Zwerger, Rev. Mod. Phys. **80**, 885 (2008); O. Morsch, and M Oberthaler, Rev. Mod. Phys. **78**, 179 (2006); A. D. Cronin, et al., Rev. Mod. Phys. **81**, 1051 (2009).

[2] M. Grifoni, and P. Hänggi, Phys. Rep. **304**, 229 (1998); F. S. Cataliotti, et al., Science **293**, 843 (2001).

[3] B. P. Anderson, and M. A. Kasevich, Science **282**, 1686 (1998).

[4] G. Alber, et al., *Quantum Information: An introduction to basic theoretical concepts and experiments*, (Springer, Berlin, 2001).

[5] F. Saif, Phys. Rep. **419**, 207 (2005); ibid **425**, 369 (2006).

[6] M. G. Raizen, Adv. At. Mol. Opt. Phys. **41**, 43 (1999).

[7] V. Giovannetti, et al., Nat. Phot. **5** 222 (2011).

[8] H. Xiong, and B. Wu, Phys. Rev. A **82**, 053634 (2010).

[9] M. Asjad, and F.Saif, Phys. Rev. A **84**, 033606 (2011).

[10] Edson D. Leonel, and Leonid A. Bunimovich, Phys. Rev. E **82**, 016202 (2010).

[11] J. M. Zhang, and W. M. Liu, Phys. Rev. A **82**, 025602 (2010).

[12] M. B. Dahan, et al., Phys. Rev. Lett. **76**, 4508 (1996); C. Petri et al., Phys. Rev. E **81**, 046219 (2010).

[13] M. Heimsoth, C. E. Creffield, and F. Sols, Phys. Rev. A **82**, 023607 (2010); A. Kenfack, et al., Phys. Rev. Lett. **100**, 044104 (2008); T. Salger, et al., Science **326**, 1241 (2009); F. Zhan, et al., Phys. Rev. A **84** 043617 (2011).

[14] A. Eckardt, et al., Phys. Rev. A **79** 013611 (2009).

[15] A. Eckardt, C. Weiss, and M. Holthaus, Phys. Rev. Lett. **95**, 260404 (2005); S. Arlinghaus, and M. Holthaus, Phys. Rev. A **81**, 063612 (2010); G. Lu, et al., Phys. Rev. A **83**, 013407 (2011).

[16] F. Grossmann, et al., Phys. Rev. Lett. **67**, 516 (1991); J. Gong, et al., Phys. Rev. Lett. **103**, 133002 (2009); S. Longhi, Phys. Rev. A **83**, 034102 (2011).

[17] A. Eckardt, et al., Phys. Rev. Lett. **95**, 200401 (2005); C. Sias, et al., Phys. Rev. Lett. **100**, 040404 (2008); C. Weiss, and H. P. Breuer, Phys. Rev. A **79**, 023608 (2009).

[18] C. E. Cerffield, Phys. Rev. Lett. **99**, 110501, (2007); C. Weiss, and N. Teichmann, J. Phys. B **42**, 031001 (2009); M. Roghani, et al., Phys. Rev. Lett. **106**, 40502 (2011).

[19] N. Poli, et al., Phys. Rev. Lett. **106**, 038501 (2011).

[20] D. Greif, et al., Phys. Rev. Lett. **106**, 145302 (2011).

[21] M. Greiner, et al., Nature **415** 39 (2002); T. Kinoshita, T. Wenger, and D. S. Weiss, Science **305**, 1125 (2004).

[22] F. Saif, I. Rehman, Phys. Rev. A **75**, 043610 (2007); K. Naseer, M. Ayub, and F. Saif, to be submitted.

[23] S. Pötting, et al., Phys. Rev. A **64**, 023604 (2001); P. Benjamin, et al., Phys. Rev. A **76**, 013420 (2007).

[24] F. Saif, Phys. Rev. E **62**, 6308 (2000).

[25] F. Saif, J. Opt B: Quant. Semiclass. Opt. **7** S116 (2005).

[26] F. Saif, Eur. Phys. J. D **39**, 87 (2006).

[27] J. M. Vogels, et al., Phys. Rev. A **56**, R1067 (1997); P. Courteille, et al., Phys. Rev. Lett. **81**, 69 (1998).

[28] D. I. Choi, and Q. Niu, Phys. Rev. Lett. **82**, 2022 (1999).

[29] B. Wu, and Q. Niu, Phys. Rev. A **64**, 061603 (2001); New. J. Phys. **5**, 104 (2003).

[30] K.Staliunas, et al., Phys. Rev. E **73**, 065603 (2006).

[31] O. Morsch, et al, Phys. Rev. Lett. **87**, 140402, (2001).

[32] M. E. Flatté, and M. Holthaus, Ann. Phys. (N. Y.) **245**, 113 (1996).

[33] G. P. Berman, and G. M. Zaslavsky, Phys. Lett. A **61**, 295 (1977).

[34] F. Saif, and M. Fortunato, Phys. Rev. A **65**, 013401 (2001).

[35] M. Ayub, et al., Eur. Phys. J. D **64** 491 (2011); arXiv:1101.0765

[36] H. P. Breuer, and M. Holthaus, Ann. Phys. **211**, 249 (1991).

[37] M. Abramowitz, and I. A. Stegun, *The Handbook of Mathematical Functions* (Dover, New York, 1970).

[38] M. Ayub, et al., J. Rus. Laser Res. **30**, 205 (2009); arXiv:1012.6011

[39] K. Drese, and M. Holthaus, Chem. Phys. **217**, 201 (1997).

[40] S. Iqbal, Q. Ann, and F. Saif, Phys. Lett. A **356**, 231 (2006).

[41] H. Lignier, et al., Phys. Rev. Lett. **99**, 220403 (2007).